Available online at www.sciencedirect.com
SCIENCE DIRECT®
ELSEVIER
Applied Surface Science 208–209 (2003) 107–112
applied surface science
www.elsevier.com/locate/apsusc

Laser ablation of polymers studied by ns-interferometry and ns-shadowgraphy measurements

M. Hauer[a], D.J. Funk[b], T. Lippert[a,*], A. Wokaun[a]

[a]*Paul Scherrer Institute, General Energy Research, 5232 Villigen PSI, Switzerland*
[b]*Los Alamos National Laboratory, DX-2, MS C920, Los Alamos, NM 87545, USA*

Abstract

The dynamic processes during ablation are studied by nanosecond-interferometry and shadowgraphy. Most commercial polymers exhibit poor laser ablation properties, therefore special triazene polymers, with superior ablation properties were developed. The photochemical active triazene group absorbs around 330 nm whereas the absorption around 200 nm is due to the photostable aromatic groups. The ns-interferometry shows that the etching of the triazene polymer starts and ends with the laser beam after irradiation at 193 and 308 nm. Shadowgraphy of the triazene polymer and polyimide reveal that the speed of the aerial shockwave increases with fluence and is higher for irradiation at 193 nm than for 308 nm. Shockwaves with equal or higher velocities are observed for the triazene polymer compared to polyimide.

Keywords: Laser ablation; Shadowgraphy; Interferometry; Reflectivity; Triazene polymer; Polyimide

1. Introduction

Laser ablation of polymers was first reported in 1982 [1,2] and has been studied using many different techniques. It has been emphasized that a better understanding of the time scale of the ablation process is fundamental for an understanding of the physical chemistry of this phenomenon. Many different approaches, such as time resolved absorption [3] and emission spectroscopy [4], time resolved Raman spectroscopy [5,6], time resolved infrared spectroscopy [7,8] and time resolved quadrupole mass spectroscopy [9–12] were used to obtain a better understanding of the ablation process, but the ablation mechanism remains still controversial [13].

Most commercial polymers exhibit poor laser ablation properties for irradiation wavelengths $\geq$248 nm. Bad ablation properties may be defined as high threshold fluences, deposition of debris, modification of the chemical and physical properties of the remaining polymer. Therefore, polymers were developed which reveal superior ablation properties for irradiation wavelengths of $\geq$308 nm [14]. The active chromophore of the triazene polymer decomposes photochemically at irradiation intensities well below the threshold of ablation [15]. The photolabile triazene group (N=N–N) is part of the polymer main chain (Fig. 1). Ablation reveals sharp ablation edges, no debris, low threshold fluence and high etch rates at low fluences [14–16]. The first absorption maximum around 200 nm is due to the photostable aromatic system. A second absorption maximum around 332 nm (with a similar absorption coefficient) can be assigned to the photolabile triazene group. The influence of the different chromophores on

* Corresponding author. Tel.: +41-56-3104076; fax: +41-56-3102485.
E-mail address: thomas.lippert@psi.ch (T. Lippert).

0169-4332/02/$ – see front matter
doi:10.1016/S0169-4332(02)01345-4

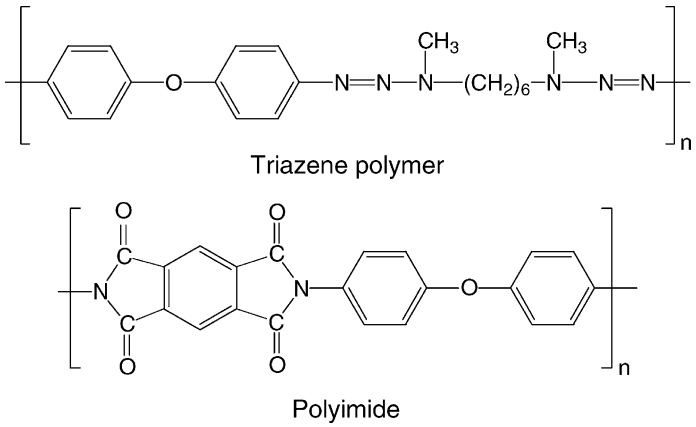

Fig. 1. Chemical structure of the triazene polymer and the polyimide.

the changes of the surface morphology during ablation can be studied by irradiating the polymer either with 193 nm (ArF) or 308 nm (XeCl). Irradiating at 308 nm is only capable of directly breaking the N–N bonds of the triazene group, whereas 193 nm can decompose the C=C bond in the aromatic system. The fast dissipation of the energy in polymer results also in N–N bond cleaving after 193 nm irradiation. The absorption coefficient of the relatively photostable (no decomposition at low intensities) polyimide at 308 nm is similar to those of the triazene polymer allowing a direct comparison between these polymers. Therefore, polyimide is used as a reference polymer (commercial, photostable) to directly compare the performance of our designed polymer. Surface interferometry and shadowgraphy are used to compare the influence of the two absorption sites in the same and the two different polymers. Both methods have the potential to give strong indications for the underlying mechanism. The ns-surface interferometry studies have shown that some polymers (nitrocellulose, polymethylmethacrylat) exhibit a pronounced swelling before ablation [17,18], whereas the ablation process of an other special designed polymer starts and ends with the laser pulse [19]. The surface swelling was attributed to a photothermal process, while the absence of swelling was used as indication for a photochemical process [16].

With shadowgraphy measurements the laser ablation induced shockwave and ejected material [3,17,20] (solid and gaseous) can be analyzed. Modeling the laser ablation induced shockwave of an energetic polymer has shown, that in some cases the expansion of the shockwave cannot be explained by the laser energy alone [21]. The decomposition enthalpy of the polymer has to be included in the modeling.

2. Experimental

The triazene polymer was prepared by a previously described method [22]. The 1–2 μm thick polymer films were spin coated from a chlorobenzene solution (10% polymer) and dried at 40 °C for 24 h. The polyimide film (75 μm thick, Kapton™ HN) was obtained from DuPont. All measurements were performed under ambient pressure at room temperature.

For the irradiation (pump laser) at 308 nm a Compex 205 XeCl excimer laser from Lambda Physik (FWHM 30 ns) was used, whereas for the irradiation at 193 nm a LPX 301i ArF excimer laser (Lambda Physik, FWHM of 25 ns) was applied. As probe laser (for both measurement setups) the 2nd harmonic of an Brillant Bω Nd:YAG laser from Quantel (FWHM of 5 ns) was used.

For the shadowgraphy experiments the optical pathway of the probe laser was modified to a Mach–Zehnder interferometer setup [23]. One beam of the interferometer passes parallel to surface of the polymer, through the ablation plume, while the other beam is unaffected by the ablation process. Both beams are recombined in a second beamsplitter where the fringe pattern is created. The compressed (i.e. ablation products and air) gases in the shockwave of the ablation have a higher refractive index than the ambient

atmosphere. A fringe shift results, which is proportional to the changes of the refractive index and path length of the probe beam through the ablation plume.

For the surface interference measurements the probe beam was used in a Michelson interferometric setup, similar to a setup describes previously [18]. The probe beam was divided by a beamsplitter (50:50) and one beam is reflected by a wedged substrate (allowing to select the reflection from the air/quartz interface). The other beam passes from the rear side of the sample through the wedged substrate and polymer and is reflected at the polymer/air interface. This has the advantage that the ejected material does not disturb the probe beam. Both beams are recombined in the beamsplitter and create an interference fringe pattern. Changes of the refraction index of the polymer will change the effective path length of the probe beam through the polymer, resulting in a shift of the interference fringes.

With both techniques fringe shift images are obtained. These images are evaluated according to a procedure described earlier [24]. Briefly, during both experiments a picture is recorded before and during/after the pump pulse. Both pictures are 2D fast Fourier transformed and reduced to the fringe information by selecting the specific peak from the fringes in the 2D FFT images and filtering all other peaks. The images are then inverse Fourier transformed into the complex space. The phase difference (Δp) between the reference and the measurement picture is then proportional to the fringe shift and thereby proportional to height changes (Δd) of the polymer surface (assuming that the refractive index n_D is constant). See Eq. (1), where λ is the probe wavelength.

$$\Delta p = 4\pi \cdot \frac{\Delta d \cdot n_D}{\lambda} \quad (1)$$

The amplitude difference between both pictures gives additional information about the reflectivity of the irradiated surface.

3. Results and discussion

3.1. Shadowgraphy

The shockwave created by laser irradiation starts with a planar expansion. This expansion changes to a stretched hemisphericaly expansion (the expansion perpendicular to the surface is faster than parallel to the surface). Only the expansion perpendicular to the surface was analyzed in this study.

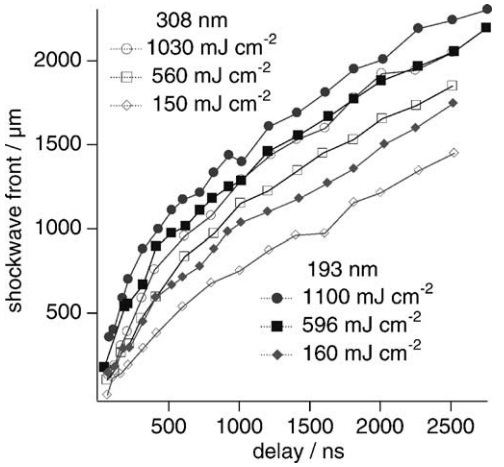

Fig. 2. The propagation of the shockwave for variable fluences after irradiation at 193 and 308 nm of the triazene polymer. The shockwave expansion is measured perpendicular to the polymer surface.

Fig. 2 shows the propagation of the shockwave created by irradiation of the triazene polymer with 308 and 193 nm. The shockwave caused by the laser ablation with 193 nm is always faster than for 308 nm irradiation. The photolabile triazene group absorbs at 308 nm. The photons at this wavelength have a quite low energy (4.02 eV) resulting in a preferential cleavage of weaker bonds in the polymer, especially the N–N bond in the triazene group.

The energy of the 193 nm photons is higher (6.59 eV) and they are absorbed in the aromatic system. These photons can break the C=C bonds and due to fast energy dissipation also other bonds in the polymer (e.g. N–N). This results in more and smaller polymer fragments, which support a faster shock wave.

Fig. 3 compares the shockwaves of the triazene polymer and polyimide after 308 nm irradiation. At the highest fluence the shockwaves of both polymers move with the same speed. As the fluence decreases the difference between both polymers becomes more and more pronounced. At 400 mJ cm^{-2} the shockwave induced by ablation of the triazene polymer is

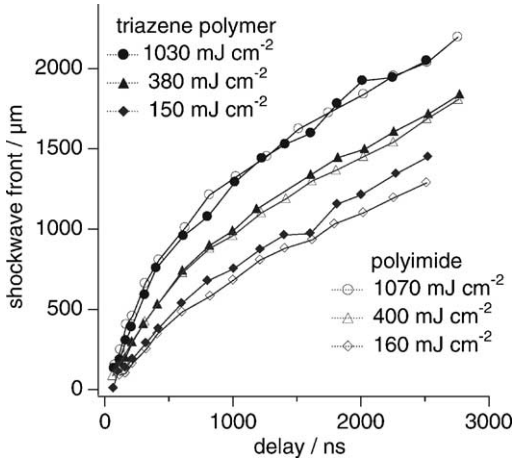

Fig. 3. The propagation of the shockwave after irradiation of the triazene polymer and polyimide at 308 nm for variable fluences. The shockwave expansion is measured perpendicular to the polymer surface.

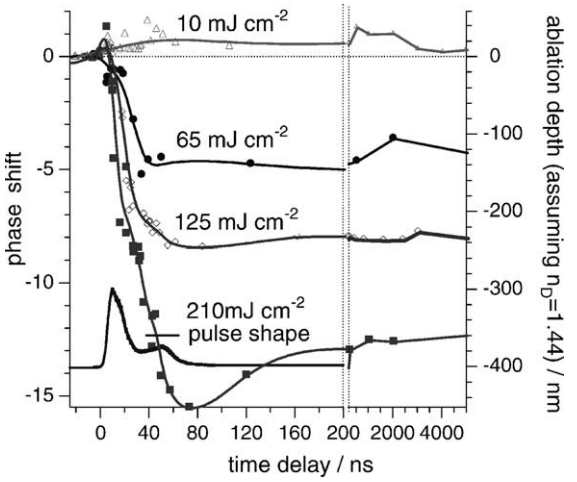

Fig. 4. Ablation depth of the triazene polymer after irradiation at 308 nm. A smoothed spline curve is added to guide the eyes along the data points. In the lower left area the relative intensity of the laser pulse is included.

only slightly faster, whereas at 150 mJ cm^{-2} the difference is quite clearly visible.

The structure of the polymer becomes more important for the lower irradiation fluences. This is also observed when the ratio of ablation rates of the triazene polymer and polyimide are compared: $d_{triazene}/d_{polyimide} = 1.3$ at 1 J cm^{-2} while for 150 mJ cm^{-2} $d_{triazene}/d_{polyimide} = 4.5$.

The difference in the ablated volume is much larger at lower fluences. Larger amounts of gaseous products are created when more material is ablated, resulting in shockwaves with higher velocities. When the differences in the ablation rates are smaller, then smaller differences in the shockwave velocities are obtained.

All observed shockwaves reveal initial propagation speeds between 970 and 2080 m s^{-1}. After 3 μs the velocity is reduced to 400–500 m s^{-1}. As the shockwave expands its volume increases and the pressure decreases accordingly. The speed of the shockwave is most probably related to the amount of gaseous products, which are formed during ablation.

3.2. Surface interference

The surface interference measurements of the triazene polymer after irradiation at 308 nm are shown in Fig. 4. The data taken at 10 mJ cm^{-2}, which is clearly below the ablation threshold of the polymer ($F_{th} = 25$ mJ cm^{-2}), show a slight swelling of the polymer surface. This swelling starts with the laser pulse and disappears after several microseconds, but no permanent swelling is observed.

At the higher laser fluences ablation is observed. At 125 mJ cm^{-2} and at 210 mJ cm^{-2} an initial positive phase shift is observed. This phase shift disappears after 10 ns and is followed by a strong negative phase shift. The positive phase shift decreases too fast to be assigned to thermal expansion of the polymer and is probably due to gas bubbles formed during the ablation process [25]. The decrease of the phase shift is attributed to ablation during the laser pulse. The ablation process ends with the end of the laser pulse.

The surface displacement for the triazene polymer after irradiation at 193 nm is shown in Fig. 5. At 10 mJ cm^{-2}, which is only slightly below the ablation threshold ($F_{th} = 12$ mJ cm^{-2}), a very weak negative phase shift is observed. This phase shift corresponds to a surface displacement of ≈20 nm and remains constant during the observed time. Measurements taken several seconds after the laser pulse reveal that this phase shift was reduced to a value corresponding to a surface displacement of ≈2 nm. At the higher fluences ablation of the polymer is observed. A short positive phase shift, similar to 308 nm irradiation (discussed earlier), is observed and followed by a negative phase

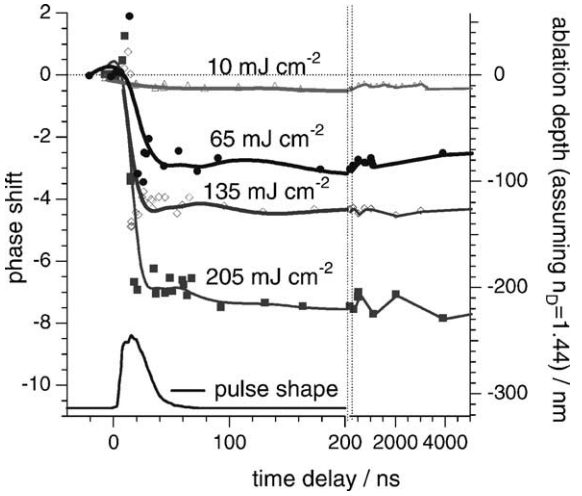

Fig. 5. Ablation depth of the triazene polymer after irradiation at 193 nm. A smoothed spline curve is added to guide the eyes along the data points. In the lower left area the relative intensity of the laser pulse is included.

shift, which is attributed to laser ablation. The etching of the polymer ends again with the laser pulse.

Fig. 6 shows the reflectivity of the triazene polymer, which changes transiently during ablation (308 nm irradiation, 125 mJ cm^{-2}). The reflectivity decreases with the laser pulse, to reach the initial reflectivity after 50 ns. No permanent changes of the reflectivity

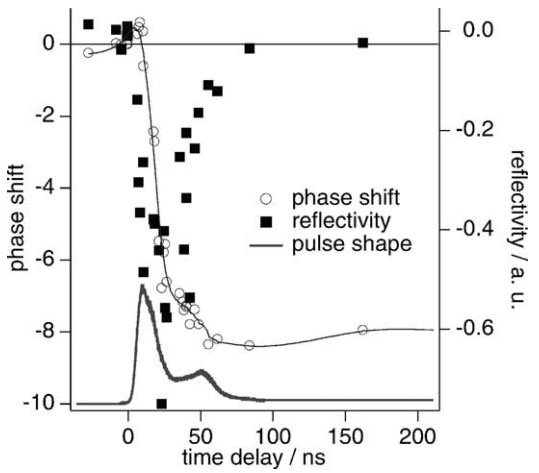

Fig. 6. Reflectivity change during the ablation process of the triazene polymer after irradiation at 308 nm with 125 mJ cm^{-2}. The intensity of the pulse and the displacement of the polymer surface have been included.

are observed, which is in agreement with surface analysis where the same chemical composition of the ablated polymer was determined after irradiation [26]. A decrease of the refractive index (n_D) of the polymer or an increase of the refractive index in front of the polymer can explain this change of the reflectivity. Other possibilities are a temporary surface roughening or products in form of micro bubbles which increase the amount of diffuse reflected light and thereby decrease the specular reflected light.

The absence of thermal swelling and the end of the ablation process with the end of the laser pulse, are strong indications, that at both wavelengths a photochemical ablation mechanism is at least partly responsible for the ablation process. The reflectivity changes during the laser ablation process indicate that the refractive index of the polymer might not be constant. This could also explain the transient positive phase shift observed prior to ablation. The absence of surface swelling, the end of ablation with the laser pulse and recovering of the reflectivity during the laser pulse strongly support a pronounced photochemical part in the laser ablation process. A comparison of the interferometry data with polyimide will show whether this behavior is unique to the designed photochemical active polymer and therefore an indication for a photochemical part in the ablation mechanism.

Surface interference measurements of polyimide were reported earlier [27], using a different experimental setup and other irradiation wavelengths. Irradiation at 248 nm revealed that the ablation starts and ends with the laser pulse. No surface swelling was observed, while for 351 nm irradiation a pronounced surface swelling was observed. This pronounced swelling was followed by ejection of large fragments, which prevent surface interference measurements. We plan to perform similar experiments with our setup (no interference from products) and additional irradiation wavelengths in the near future.

4. Conclusion

The shadowgraphy measurements for polyimide and the triazene polymer reveal that the speed of the shockwave increases with laser fluence and that higher shockwave speeds are obtained after irradiation at 193 nm compared to 308 nm irradiation. An

increase of the laser fluence results in an increase of the amount of ablated material and therefore in an increase of the shockwave velocity. The 193 nm photons have higher photon energies and are capable of breaking more bonds in the polymer e.g. decomposition of the phenyl group. This results in more and smaller gaseous fragments and therefore a higher shockwave velocity.

The ns-interferometry shows that the ablation of the triazene polymer starts and ends with the laser pulse. The initially observed positive phase shift is too short to be assigned to thermal swelling. Therefore, we suggest that this phase shift is attributed to micro bubbles inside the polymer, which are created during the ablation process. The negative phase shift is assigned to ablation of the polymer. After the laser pulse the phase shift remains constant and corresponds to the ablation depth measured with a surface profilometer. The reflectivity decreases during the laser pulse. This decrease shows that the laser light has an effect on the physical properties of the polymer or that products are formed inside the polymer. The data strongly support a pronounced photochemical part in the ablation mechanism of the triazene polymer.

Acknowledgements

This work has been supported by the Swiss National Science Foundation. We wish to thank Professor Masuhara for valuable discussions.

References

[1] R. Srinivasan, V. Mayne-Banton, Appl. Phys. Lett. 576 (1982) 41.
[2] Y. Kawamura, K. Toyoda, S. Namba, Appl. Phys. Lett. 374 (1982) 40.
[3] H. Fukumura, E. Takahashi, H. Masuhara, J. Phys. Chem. A. 750 (1995) 99.
[4] H. Fujiwara, H. Fukumoto, H. Fukumura, H. Masuhara, Res. Chem. Intermed. 879 (1998) 24.
[5] D.E. Hare, D.D. Dlott, Appl. Phys. Lett. 715 (1994) 64.
[6] D.E. Hare, J. Franken, D.D. Dlott, J. Appl. Phys. 5950 (1995) 77.
[7] T. Lippert, P.O. Stoutland, Appl. Surf. Sci. 43 (1997) 109–110.
[8] T. Lippert, A. Koskelo, P. Stoutland, J. Am. Chem. Soc. 1551 (1996) 118.
[9] T. Lippert, A. Wokaun, S.C. Langford, J.T. Dickinson, Appl. Phys. A. 655 (1999) 69.
[10] T. Lippert, S.C. Langford, A. Wokaun, G. Savas, J.T. Dickinson, Appl. Phys. A. 7116 (1999) 89.
[11] M. Hauer, J.T. Dickinson, S.C. Langford, T. Lippert, A. Wokaun, Appl. Surf. Sci. 197–198 (2002) 791.
[12] D.J. Krajnovich, J. Phys. Chem. A. 1175 (1996) 101.
[13] D. Bäuerle, Laser Processing and Chemistry, 3rd ed., Springer, Heidelberg, 2000.
[14] J. Wei, N. Hoogen, T. Lippert, O. Nuyken, A. Wokaun, J. Phys. Chem. B 1267 (2001) 105.
[15] T. Lippert, C. David, J.T. Dickinson, M. Hauer, U. Kogelschatz, S.C. Langford, O. Nuyken, C. Phipps, J. Robert, A. Wokaun, J. Photochem. Photobiol. A. 87 (2001) 145.
[16] Th. Lippert, A. Wokaun, J. Stebani, O. Nyken, J. Ihlemann, Angew. Macromol. Chem. 97 (1993) 206.
[17] H. Furutani, H. Fukumura, H. Masuhara, S. Kambara, T. Kitaguchi, H. Tsukada, T. Ozawa, J. Phys. Chem. B. 3395 (1998) 102.
[18] H. Furutani, H. Fukumura, H. Masuhara, Appl. Phys. Lett. 3413 (1994) 65.
[19] H. Furutani, H. Fukumura, H. Masuhara, T. Lippert, A. Yabe, J. Phys. Chem. A. 5742 (1997) 101.
[20] R. Srinivasan, Appl. Phys. A. 417 (1993) 56.
[21] L.S. Bennett, T. Lippert, H. Furutani, H. Fukumura, H. Masuhara, Appl. Phys. A. 327 (1996) 63.
[22] J. Stebani, O. Nuyken, T. Lippert, A. Wokaun, Makromol. Chem. Rapid Commun. 2943 (1993) 206.
[23] D. Breitling, H. Schittenhelm, P. Berger, F. Dausinger, H. Hügel, Appl. Phys. A. S505 (1999) 69.
[24] M. Takeda, H. Ina, S. Kobayashi, J. Opt. Soc. 156 (1982) 72.
[25] R. Srinivasan, K.G. Casey, B. Braren, M. Yeh, J. Appl. Phys. 1604 (1990) 67.
[26] T. Lippert, T. Nakamura, H. Niino, A. Yabe, Macromol. 6301 (1996) 29.
[27] T. Masubuchi, T. Tada, E. Nomura, K. Hatana, H. Fukumura, H. Masuhara, J. Phys. Chem. A 2180 (2002) 106.